Interdiscip Sci Comput Life Sci (2016) 8:403–411
DOI 10.1007/s12539-015-0121-z

ORIGINAL RESEARCH ARTICLE

Computational Analysis and Binding Site Identification of Type III Secretion System ATPase from *Pseudomonas aeruginosa*

Raju Dash[1] · S. M. Zahid Hosen[2] · Tasniha Sultana[1] · Md. Junaid[3] · Mohuya Majumder[1] · Ismat Ara Ishat[1] · Mir Muhammad Nasir Uddin[4]

Received: 21 March 2015 / Revised: 10 June 2015 / Accepted: 16 July 2015 / Published online: 15 August 2015

Abstract In many gram-negative bacteria, the type III secretion system (T3SS), as a virulence factor, is an attractive target for developing novel antibacterial. Regarding this, in our study, we aimed to identify the putative drug target for *Pseudomonas aeruginosa*, considering ATPase enzyme involved in the type III secretion system. Selective protein sequence of *P. aeruginosa* involved in the T3SS was retrieved from NCBI databases, and its homologues were subjected to phylogenetic analysis. Its association in T3SS was analyzed via STRING, and the 3D structure was determined by means of homology modeling followed by intensive optimization and validation. The binding site was predicted by 3DLigandSite and examined through molecular docking simulation by Autodock Vina with salicylidene acylhydrazide class of virulence-blocking compounds. PROCHECK analysis showed that 96.7 % of the residues were in the most favored regions, 1.9 % were in the additional allowed region, and 1.4 % were in the generously allowed region of the Ramachandran plot. The refined model yielded ERRAT scores of 88.124 and Verify3D value of 0.2, which indicates that the environmental profile of the model is good. The best binding affinity was observed by ME0055 compound, and ALA160, ALA161, GlY162, GLY163, GLY164, GLY165, SER166, THR167, TYR338, and PRO339 residues were found to be having complementary in the ligand-binding site. However, these findings should be further confirmed by wet lab studies for design a targeted therapeutic agent.

Keywords ATPase · *Pseudomonas aeruginosa* · Type III secretion system · Phylogenetic analysis · Salicylidene acylhydrazide

✉ Mir Muhammad Nasir Uddin
nasirmir@cu.ac.bd

Raju Dash
rajudash.bgctub@gmail.com

S. M. Zahid Hosen
pharmacistsmzh.bcsir@gmail.com

Tasniha Sultana
tasniha36@gmail.com

Md. Junaid
md.junaid@northsouth.edu

Mohuya Majumder
mohuyamojumdar.bgctub@gmail.com

Ismat Ara Ishat
ismataraishat@gmail.com

[1] Department of Pharmacy, BGC Trust University Bangladesh, Chittagong 4000, Bangladesh

[2] Drugs and Toxins Research Division, Bangladesh Council of Scientific and Industrial Research (BCSIR), Chittagong 4220, Bangladesh

[3] Department of Pharmaceutical Sciences, North South University, Dhaka 1229, Bangladesh

[4] Department of Pharmacy, University of Chittagong, Chittagong 4331, Bangladesh

1 Introduction

Over the past several decades, occurrences of antimicrobial-resistant infections have dramatically increased and associated with adverse patient outcomes [1]. Substitute approach to combat infection is critical and has resulted the introduction of more specific drugs targeted at particular bacterial virulence systems or essential regulatory pathways [2]. In gram-negative pathogen, one of the most common protein delivery machines is the type III secretion

system (T3SS), a fascinating system that comprised a needle-like injection system which simplifies the secretion of effector molecules directly into the mammalian host epithelium [3]. In *Pseudomonas aeruginosa*, the T3SS was discovered in 1996 [4] and since 36 genes have been found to be associated with T3SS function [5]. The active type III cytotoxin secretion of *P. aeruginosa* targets host immune cells, e.g., macrophage and neutrophils, allowing the organisms to evade the immunologic response and sometimes lowering the variety of viable host defense cells [6]. Only four effectors, named ExoS, ExoT, ExoU, and ExoY, have been identified in *P. aeruginosa*, where ExoU is the most potent cytotoxin [7]. The entire secretion machine is made of over 20 different proteins called the Psc, Pop, or Pcr components, where the needle-like structure is central to the injection process [8], and a set of three proteins mamed PopB, PopD, and PcrV in *P. aeruginosa* is also crucial to establish a pore into the membrane of eukaryotic cells [9, 10]. However, these machines require a component, typically an ATPase, which provides energy to the process [11]. Due to concern of any future therapeutic cross-reaction with human enzymes, current approaches for T3SS inhibition strategies do not explicitly target the T3SS ATPases. On the other hand, the bacterial enzymes have <25 % identity to human ATPases, and also the active sites showed the significant differences between bacterial and human enzymes [12]. Since a number of recent studies have been focused on bacterial ATPases [12–14], that is why, in our present study, we aimed to identify the favorable binding sites and the key residues responsible for substrate specificity of T3SS ATPase enzyme from *P. aeruginosa* using various bioinformatics models and docking studies [15].

2 Result

2.1 Sequence Retrieval and Sequence Analysis

Protein sequences were retrieved from the GenBank through BlastP [16] algorithm with *E* value <0.01, at the National Centre for Biotechnology Information (NCBI) using the BAP51534.1 sequence as query, and several T3SS ATPase orthologs from different families of bacteria were selected for further analysis. Sequences were aligned using the ClustalW program (http://www.ebi.ac.uk) using default parameters. Neighbor-joining tree was constructed with MEGA6.0 software, using the UPGMA method with the following parameters: Dayhoff amino acid replacement model; uniform rates of site-specific mutation; and complete deletion of gaps and missing data (Fig. 1). The phylogeny was evaluated using the bootstrap method with 1000 replications.

2.2 Analysis of Physicochemical Properties and Interacting Networks

Analysis of physicochemical properties using ProtParam revealed that the protein had 30,160 extinction coefficient, 48.12 instability index, 96.43 aliphatic index, −0.172 grand average of hydrophobicity, and also had more positively charged residues than negative-charged amino acids. The interacting partners of protein that are under investigation were determined by using STRING (Fig. 2). The results were predicted with the highest confidence score 0.900.

2.3 Analysis of Secondary Structure and Model Building

The secondary structure of the current protein was predicted by SOPMA, which correctly predicts the amino acids for a three-state description of the secondary structure in alpha helix, beta sheet, and random coil, shown in Table 1. The three-dimensional structure of pscN ATPase protein was predicted by using the PHYRE2. In intensive mood, 420 residues (98 %) of pscN ATPase were modeled at >90.0 % confidence by the single highest scoring template. First the pscN ATPase was searched against the Protein Data Bank (PDB). The best template structure was selected based on the sequence homology. Here, 2DPY_-Chain A, crystal structure of the flagellar type III ATPase flii domain showed the highest similarity to the pscN ATPase protein of *P. aeruginosa*. The template similarity was 45 %, and remaining protein sequence was structured by the principle of domain analysis. For further refinement to determine the high-resolution structure of the protein, ModRefiner was used.

2.4 Model Validation

For rationalization of the predicted structure, Ramachandran plot analysis was done by PROCHECK [17] server. The results of this analysis are depicted in Fig. 3a. The selected model was then verified by using ERRAT, Verify 3D [18]. This model was also verified by QMEAN and PROSA II and is shown in Fig. 3b, c.

2.5 Molecular Docking Studies

The predicted binding site from 3DLigandSite is shown in Fig. 4a. Docking study of the compounds with pscN ATPase revealed that ME0055 (Fig. 4b) had the binding affinity −7.4 kcal/mol and ME0052 (Fig. 4c) −7.0 kcal/-mol, having the root-mean-square deviation (RMSD) value 0.00, respectively. The post-docking analysis of ME0055 and ME0052 is shown in Fig. 4d, e.

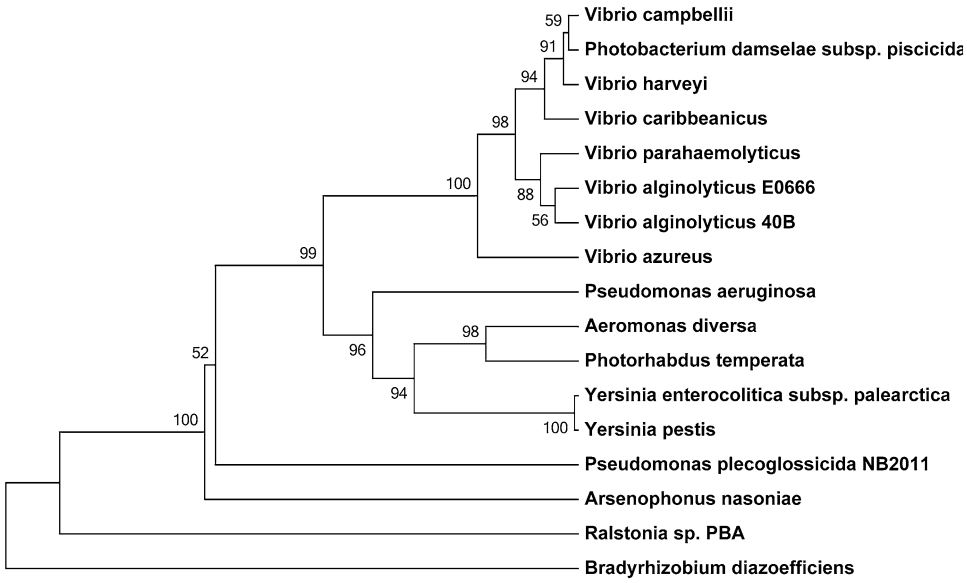

Fig. 1 Phylogeny of T3SS ATPases was inferred by using neighbor-joining method of the MEGA6.0 software. A total of 17 protein sequences were used for analysis from the following bacterial species: *Pseudomonas aeruginosa* (BAP51534.1), *Aeromonas diversa* (WP_005347922.1), *Yersinia enterocolitica* (ADZ44455.1), *Yersinia pestis* (WP_016597357.1), *Photorhabdus temperata* (WP_021323777.1), *Vibrio harveyi* (WP_005450237.1), *Vibrio campbellii* (WP_005528939.1), *Vibrio azureus* (WP_021711596.1), *Vibrio alginolyticus* (WP_005395117.1), *Photobacterium damselae* (AAU11472.1), *Vibrio caribbeanicus* (EFP95875.1), *Vibrio parahaemolyticus* (WP_015296797.1), *Vibrio tubiashii* (EGU53832.1), *Vibrio alginolyticus* (EEZ81818.1), *Pseudomonas plecoglossicida* (WP_016394485.1), *Arsenophonus nasoniae* (CBA72162.1), Ralstonia sp., PBA (EIZ05353.1), and *Bradyrhizobium diazoefficiens* (BAR63297.1)

3 Discussion

In recent years, the investigation for non-antibiotic treatments of infectious diseases has gained more consideration [19]. Therefore, the rational antivirulence drug design and inhibiting the transport facility of the virulence system is a new strategy of current antimicrobial drug development [20, 21]. The strategy of our study was to target pscN ATPase as a type III secretion system blocker. Regarding this, protein sequences were retrieved from NCBI databases through BlastP-based homologous searching, and phylogenetic analysis of identified T3SS ATPase orthologs from different bacterial strains was performed to establish their evolutionary profile. As shown in neighbor-joining phylogenetic tree (Fig. 1), pscN ATPase of *Pseudomonas arugenosa* showed the highest amino acid sequence identity to other T3SS ATPases including *Aeromonas diversa* WP_005347922.1 (83.92 %), *Yersinia enterocolitica* ADZ44455.1 (83.66 %), *Yersinia pestis* WP_016597357.1 (83.29 %), *Photorhabdus temperata* WP_021323777.1 (83.22 %), *Vibrio harveyi* WP_005450237.1 (79.25 %), *Vibrio campbellii* WP_005528939.1 (79.02 %), *Vibrio azureus* WP_021711596.1 (79.49 %), *Vibrio alginolyticus* WP_005395117.1 (79.49 %), *Photobacterium damselae* AAU11472.1 (79.02 %), *Vibrio caribbeanicus* EFP95875.1 (78.79 %), *Vibrio parahaemolyticus* WP_015296797.1 (78.55 %), *Vibrio tubiashii* EGU53832.1 (79.32 %), *Vibrio alginolyticus* EEZ81818.1 (78.55 %), *Pseudomonas plecoglossicida* WP_016394485.1 (74.83 %), *Arsenophonus nasoniae* CBA72162.1 (71.56 %), Ralstonia sp., PBA EIZ05353.1 (64.34 %), and *Bradyrhizobium diazoefficiens* BAR63297.1 (60.09 %). Proteins having similar profiles will often be inferred to be functionally related within the postulation that proteins mixed up in same metabolic pathway or cellular system will likely are co-inherited during evolution [22]. Phylogenetic analysis of the T3SS ATPase enzymes among 17 taxa of different bacterial genus indicated that most variation in enzyme is due to evolutionary distance and may be non-adaptive, and also it had been appreciably observed that diverse of T3SS ATPases often share the same substrates. As sequence homology is certainly not a definitive argument to describe the precise enzymatic activity of T3SS ATPase, the functional depiction of these enzymes remains compulsory. In order to gain a better understanding of the molecular profile, analysis through ProtParam was conducted in respect of different parameters to obtain the physicochemical properties of protein. According to the result, this protein has a high extinction coefficient and low instability index. The protein also exhibits thermostability, since it has high aliphatic index. Again, it also reveals the negative GRAVY with molecular weight of 46,759.4 and pI 6.35. As we conceived

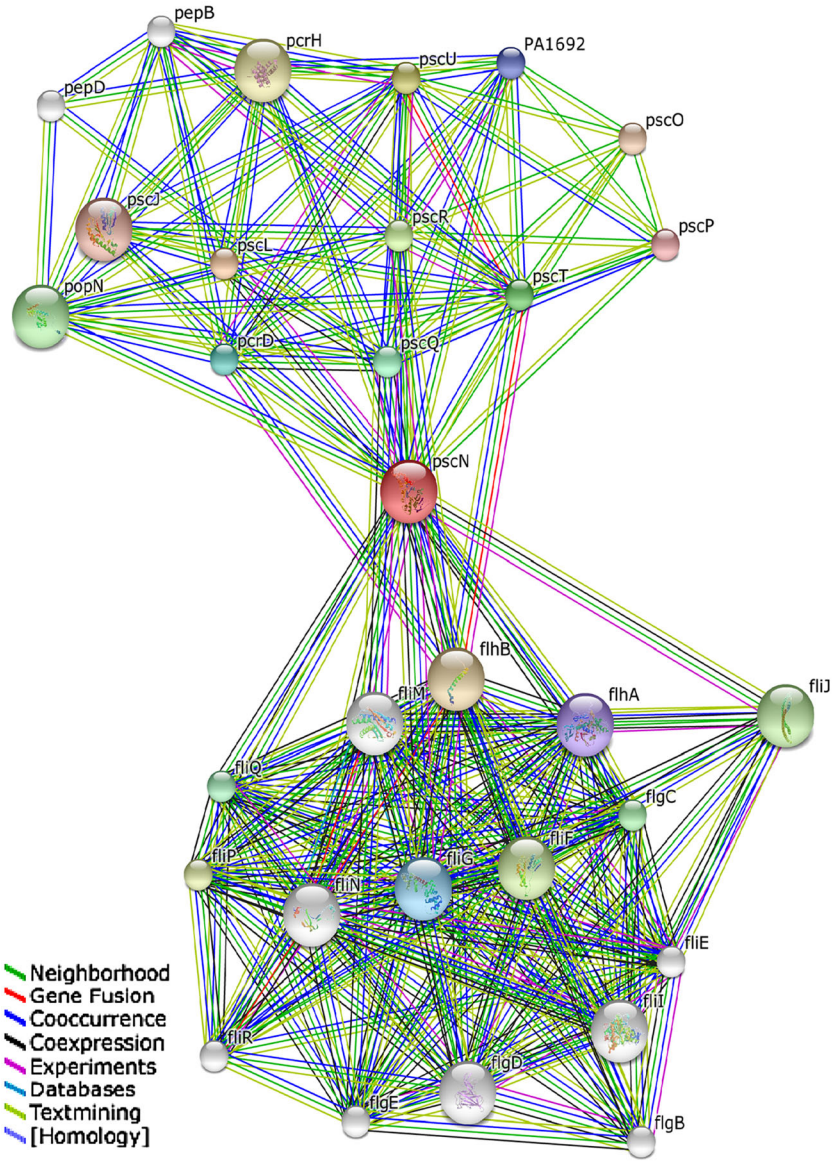

Fig. 2 Protein–protein interaction network of pscN ATPase. Network was generated from STRING database, and edges represented in *colored lines* between the proteins indicate various types of interaction evidence. Protein nodes, which are enlarged, indicate the availability of 3D protein structure information

Table 1 Computed secondary structure elements of pscN ATPase protein by SOMPA

Structure	Number of residues	Percentage (%)
Alpha helix [Hh]	225	52.45
3_{10} helix [Gg]	0	0.00
Pi helix [Ii]	0	0.00
Beta bridge [Bb]	0	0.00
Extended strand [Ee]	51	11.89
Beta turn [Tt]	39	9.09
Bend region [Ss]	0	0.00
Random coil [Cc]	114	26.57
Ambiguous states [?]	0	0.00
Other states	0	0.00

that inhibitor should target bacterial ATPases concerned in the transport process of T3SS, we used a systems biology approach to validate the study protein. Generally, appropriate execution of a protein requires interaction with other proteins, where protein–protein interactions encompass a critical role in functions and the structural organization of a cell [23]. Interaction of pscN ATPase with its partner proteins was determined through STRING, shown in Fig. 2. With highest confidence score, STRING predicted that pscN ATPase is associated with some translocation proteins in type III secretion such as pscL, pscR, pscQ, pscP, pscT, pscO, and pscU. Network analysis also showed that it interacts with secretory apparatus protein, type III export protein, regulatory protein and also flagellar biosynthesis

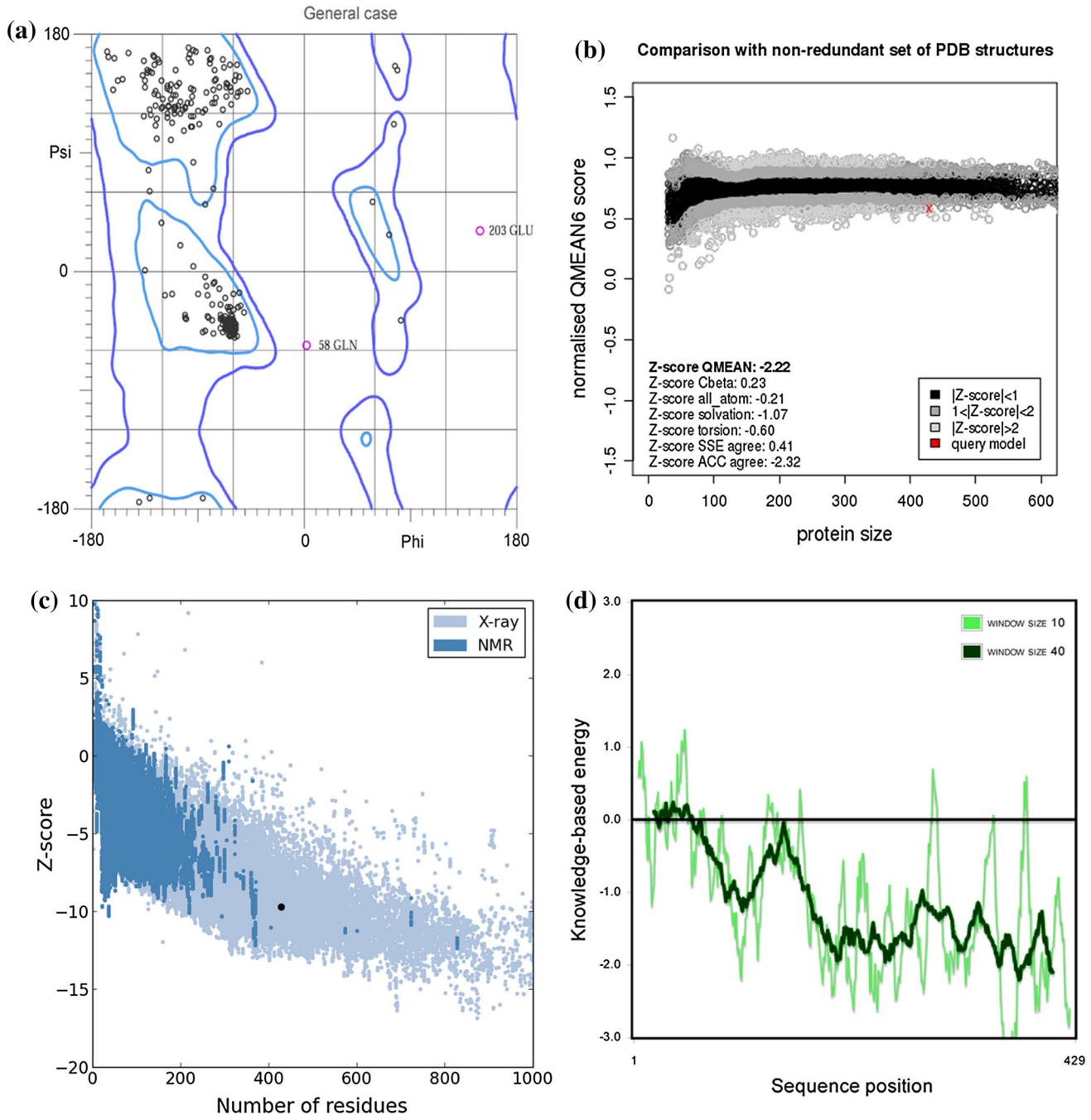

Fig. 3 Structural quality assessment pscN ATPase protein. **a** Ramachandran plot. **b** QMEAN scores and comparison plot with non-reductant set of PDB structures, and good models are generally located in the *dark zone*. **c** ProSA-web *z*-scores of all protein chains in PDB determined by X-ray crystallography (*light blue*) or NMR spectroscopy (*dark blue*) with respect to their length. **d** Local model quality obtained from PROSAII with respect to sequence position

protein, which confirmed that targeting this enzyme will disrupt the mechanism of type III secretion system. It is commonly believed that the functionalities of a protein can be determined by their unique three-dimensional structures, which are determined by the exact spatial position of each atom [24]. Therefore, we subjected secondary structure analysis of our current protein by the self-optimized prediction method with alignment (SOPMA) and revealed that it contains 52.45 % alpha helix, 11.89 % extended strand, and 26.57 % random coil (Table 1). In proteomics, the most important part is to determine the 3D structure of a protein [25]. In our study, PHYRE2 was used to generate theoretical structure of pscN ATPase with >90.0 % confidence match which implies that overall fold of the model was

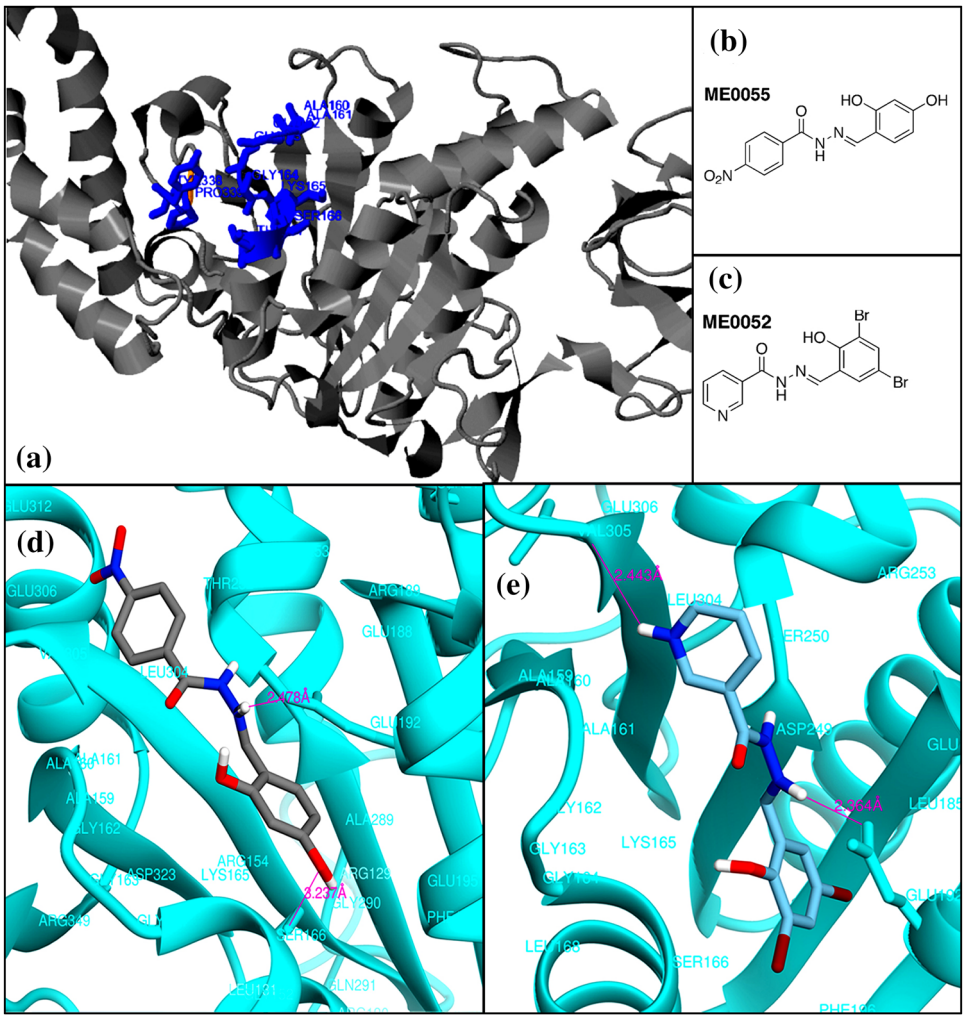

Fig. 4 Active site determination and docking analysis of pscN ATPase protein. **a** The *blue colors* indicate the most potent active site's residues, generated from 3DLigandSite. 2D structure of **b** ME0055 and **c** ME0052 and analysis of **d** ME0055- and **e** ME0052-docked complex obtained from Autodock Vina. The ligand molecules is shown as stick, protein as cartoon, and H-bonds as *pink lines*

almost certainly correct and the central core of the model tends to be accurate [26]. According to results from PHYRE2, the protein contains 15 % disorder, 37 % alpha helix, and 21 % beta strand. The conserved domain database (CDD) [27] predicted that ALA160, ALA161, GLY162, GLY163, GLY164, LYS165, and SER166 of motif A residues are involved in ATP-binding site. To get a more accurate structure, we used ModRefiner to refine our current study protein. After derivation by the ModRefiner, the protein was subjected to verify through PROCHECK, WHATCHECK, ERRAT, PROVE, Verify3D, QMEAN, and PROSA II analysis. PROCHECK created Ramachandran plot which showed the distribution of φ and ψ angle in the model, shown in Fig. 3a. According to the plot statistics, 96.7 % of residues were located in the most favored region, 1.4 % in outlier region, and 1.9 % generously allowed region. As for a good-quality model, the residues located in the core and allowed regions should be over 90 %, which is the case for the model presented here (since 96.7 % + 1.4 % = 98.1 %) [28]. Verification was also done with Verify3D model, ERRAT, where ERRAT showed that overall quality factor 88.124 and can be considered as a good model. Verify3D graph indicated that the environment profile of the model 90.21 % of the residues had an averaged 3D-1D good score of 0.2. The PROSA II and QMEAN analysis showed the z-score of −8.33 (Fig. 3c) and −2.22 (Fig. 3b), respectively. QMEAN [29] score ranging between 0 and 1 and higher value reflects the better quality of input model, where the score of the present model was 0.580. From the results of the entire structural validation programs, it was inferred that the homology modeled protein is reliable for further study. For understanding enzyme–substrate interaction, we had docked the model of pscN ATPases with selected substrates using Auto Dock Vina. The salicylidene acylhydrazides have been widely reported to block the function of the type three secretion system of several gram-negative pathogens and are also known as a class of anti-virulence compounds [30, 31]. Though the virulence-blocking activity of this class of compounds had been published in various literatures [32, 33], their activity on ATPase has not been yet reported. So, for our growing interest, we had selected two salicylidene acylhydrazide class

compounds reported in Wang et al. [34] and considered for further study. Since ME0055 had the higher negative and low value of free energy of binding, it indicated a strong favorable bond between pscN ATPase and in most favorable conformations. The active site identification by 3DLigandSite [35] predicted that ALA160, ALA161, GlY162, GLY163, GLY164, GLY165, SER166, THR167, TYR338, and PRO339 are involved in ligand-binding site (shown in Fig. 4a), and these residues were found to have similar in both ME0052- and ME0055-binding sites (shown in Fig. 4e, d). In addition, GLU192 was also involved in catalytic action, as it formed hydrogen bonds with both ME0052 and ME0055 compounds. Post-docking analysis is also suggested that ME0055 compound formed a salt bridge with one of the active binding site's residue SER166 with bonding distance 3.237 Å, which further confirmed that it has relevant activity on pscN ATPase.

In a summary, in order to ensure the correct order of export, a substantial number of checkpoints are involved in type III secretion system, where the respective ATPase plays a critical role. Nevertheless, the lack of the structural information about this enzyme hinders the detailed characterization of its biological functions and applications in structure-based drug designing of virulence-blocking agents. This study is useful to extend novel therapeutics for many other T3SS-encoding pathogens, though further in vivo validation and conformation of the present finding is required.

4 Experimental Section

4.1 Sequence Retrieval, Multiple Sequence Alignment and Phylogenetic Analysis

A sequence of ATPase enzyme involved in type III secretion system from *P. aeruginosa* (pscN ATPase) was retrieved from the NCBI databases, the accession ID of ATPase is BAP51534, and it contains 429 amino acids. BlastP [16] (www.ncbi.nlm.nih.gov/BLAST/) was used to search for its homologous, selected T3SS ATPase sequences from other genus were multiply aligned using ClustalW, and a phylogenetic tree was generated from the structural alignment with MEGA6.0 [36] using the UPGMA method.

4.2 Analysis of Physiochemical Properties and Interacting Networks

ExPasy's ProtParam [37] tool was utilized to calculate the physicochemical characteristics of the protein, and STRING [38] was used to identify the networking partners of pscN ATPase. The STRING is a biological database which is used to build network of protein–protein interaction for different known and predicted protein interactions.

4.3 Analysis of Secondary Structure and 3D Model Building

Secondary structural properties of the protein were calculated by using self-optimized prediction method with alignment (SOPMA) [39], and its 3D homology model was built by the most popular online protein fold recognition server PHYRE2 [26], and ModRefiner [40] was used to refine the predicted model.

4.4 Evaluation and Validation of Model

The accuracy and the stereo chemical quality of the predicted model was evaluated with PROCHECK [17] by Ramachandran plot analysis [41], Verify3D [42], ERRAT [43], PROVE [44], QMEAN [29], and PROSA II [45].

4.5 Docking Simulation Study

ME0052 and ME0055 compounds were selected for this study, shown in Fig. 4b, c. Compounds were drawn in Symyx Draw 4.0 and then prepared for docking using the Sybyl 7.3 Molecular Modeling Suite of Tripos, Inc. 3D conformations were generated using Concord 4.0 [46]. Hydrogen atoms were added, and charges were loaded using the Gasteiger and Marsili charge calculation method [47]. The ligands were minimized with the Tripos force field prior to dock, using the Powell method with an initial Simplex [48] optimization and 1000 iterations or gradient termination at 0.01 kcal/(mol*A). The hypothetical protein was prepared by using dock preparation wizard integrated in UCSF Chimera [49], by adding hydrogen and charges [50], and also 3DLigandSite [35] was used to predict the binding site. Input ligand file format was mol2, so these were further converted into pdbqt format by Python Molecular Viewer with AutoDock tools, required by AutoDockVina [51]. The size of grid box in AutoDock Vina was kept at 63.6088, 77.5960, and 50.5972, respectively, for *X*, *Y*, and *Z*. The energy range was kept at 4 which was default setting. Autodock Vina was implemented through shell script provided by AutoDock Vina developers. The binding affinity of ligand was observed by Kcal/Mol as a unit for a negative score [52].

References

1. Aminov RI (2009) The role of antibiotics and antibiotic resistance in nature. Environ Microbiol 11:2970–2988
2. Lynch SV, Wiener-Kronish JP (2008) Novel strategies to combat bacterial virulence. Curr Opin Crit Care 14(593–599):3
3. Roy-Burman A, Savel RH, Racine S, Swanson BL, Revadigar NS, Fujimoto J, Sawa T, Frank DW, Wiener-Kronish JP (2001)

Type III protein secretion is associated with death in lower respiratory and systemic *Pseudomonas aeruginosa* infections. J Infect Dis 183:1767–1774
4. Yahr TL, Goranson J, Frank DW (1996) Exoenzyme S of *Pseudomonas aeruginosa* is secreted by a type III pathway. Mol Microbiol 22:991–1003
5. Brutinel ED, Vakulskas CA, Brady KM, Yahr TL (2008) Characterization of ExsA and of ExsA-dependent promoters required for expression of the *Pseudomonas aeruginosa* type III secretion system. Mol Microbiol 68:657–671
6. Finck-Barbancon V, Goranson J, Zhu L, Sawa T, Wiener-Kronish JP, Fleiszig SM, Wu C, Mende-Mueller L, Frank DW (1997) ExoU expression by *Pseudomonas aeruginosa* correlates with acute cytotoxicity and epithelial injury. Mol Microbiol 25:547–557
7. Sato H, Frank DW (2004) ExoU is a potent intracellular phospholipase. Mol Microbiol 53:1279–1290
8. Blocker AJ, Deane JE, Veenendaal AK, Roversi P, Hodgkinson JL, Johnson S, Lea SM (2008) What's the point of the type III secretion system needle? Proc Natl Acad Sci USA 105:6507–6513
9. Dacheux D, Goure J, Chabert J, Usson Y, Attree I (2001) Pore-forming activity of type III system-secreted proteins leads to oncosis of *Pseudomonas aeruginosa*-infected macrophages. Mol Microbiol 40:76–85
10. Goure J, Pastor A, Faudry E, Chabert J, Dessen A, Attree I (2004) The V antigen of *Pseudomonas aeruginosa* is required for assembly of the functional PopB/PopD translocation pore in host cell membranes. Infect Immun 72:4741–4750
11. Filloux A (2011). Protein secretion systems in *Pseudomonas aeruginosa*: an essay on diversity, evolution, and function. Front Microbiol 2:155
12. Swietnicki W, Carmany D, Retford M, Guelta M, Dorsey R, Bozue J, Lee MS, Olson MA (2011) Identification of small-molecule inhibitors of Yersinia pestis Type III secretion system YscN ATPase. PLoS One 6:18
13. Yoshida Y, Miki T, Ono S, Haneda T, Ito M, Okada N (2014) Functional characterization of the type III secretion ATPase SsaN encoded by Salmonella pathogenicity island 2. PLoS One 9:e94347
14. Wilharm G, Dittmann S, Schmid A, Heesemann J (2007) On the role of specific chaperones, the specific ATPase, and the proton motive force in type III secretion. Int J Med Microbiol 297:27–36
15. Dash R, Emran TB, Uddin MM, Islam A, Junaid M (2014) Molecular docking of fisetin with AD associated AChE, ABAD and BACE1 proteins. Bioinformation 10:562–568
16. Altschul SF, Gish W, Miller W, Myers EW, Lipman DJ (1990) Basic local alignment search tool. J Mol Biol 215:403–410
17. Laskowski RA, Rullmannn JA, MacArthur MW, Kaptein R, Thornton JM (1996) AQUA and PROCHECK-NMR: programs for checking the quality of protein structures solved by NMR. J Biomol NMR 8:477–486
18. Bowie JU, Luthy R, Eisenberg D (1991) A method to identify protein sequences that fold into a known three-dimensional structure. Science 253:164–170
19. Spellberg B, Guidos R, Gilbert D, Bradley J, Boucher HW, Scheld WM, Bartlett JG, Edwards J Jr (2008) The epidemic of antibiotic-resistant infections: a call to action for the medical community from the Infectious Diseases Society of America. Clin Infect Dis 46:155–164
20. Keyser P, Elofsson M, Rosell S, Wolf-Watz H (2008) Virulence blockers as alternatives to antibiotics: type III secretion inhibitors against Gram-negative bacteria. J Intern Med 264:17–29
21. Martin CA, Hoven AD, Cook AM (2008) Therapeutic frontiers: preventing and treating infectious diseases by inhibiting bacterial quorum sensing. Eur J Clin Microbiol Infect Dis 27:635–642
22. Jothi R, Przytycka TM, Aravind L (2007) Discovering functional linkages and uncharacterized cellular pathways using phylogenetic profile comparisons: a comprehensive assessment. BMC Bioinformatics 8:173
23. Arifuzzaman M et al (2006) Large-scale identification of protein-protein interaction of Escherichia coli K-12. Genome Res 16:686–691
24. Chou KC (2004) Structural bioinformatics and its impact to biomedical science. Curr Med Chem 11:2105–2134
25. Hasan MA, Alauddin SM, Al Amin M, Nur SM, Mannan A (2014) In silico molecular characterization of cysteine protease YopT from Yersinia pestis by homology modeling and binding site identification. Drug Target Insights 8:1–9
26. Kelley LA, Sternberg MJ (2009) Protein structure prediction on the Web: a case study using the Phyre server. Nat Protoc 4:363–371
27. Marchler-Bauer A et al (2015) CDD: NCBI's conserved domain database. Nucleic Acids Res 43:20
28. Hollingsworth SA, Karplus PA (2010) A fresh look at the Ramachandran plot and the occurrence of standard structures in proteins. Biomol Concepts 1:271–283
29. Benkert P, Tosatto SC, Schomburg D (2008) QMEAN: a comprehensive scoring function for model quality assessment. Proteins 71:261–277
30. Negrea A, Bjur E, Ygberg SE, Elofsson M, Wolf-Watz H, Rhen M (2007) Salicylidene acylhydrazides that affect type III protein secretion in Salmonella enterica serovar typhimurium. Antimicrob Agents Chemother 51:2867–2876
31. Duncan MC, Linington RG, Auerbuch V (2012) Chemical inhibitors of the type three secretion system: disarming bacterial pathogens. Antimicrob Agents Chemother 56:5433–5441
32. Nordfelth R, Kauppi AM, Norberg HA, Wolf-Watz H, Elofsson M (2005) Small-molecule inhibitors specifically targeting type III secretion. Infect Immun 73:3104–3114
33. Kauppi AM, Nordfelth R, Uvell H, Wolf-Watz H, Elofsson M (2003) Targeting bacterial virulence: inhibitors of type III secretion in Yersinia. Chem Biol 10:241–249
34. Wang D et al (2011) Identification of bacterial target proteins for the salicylidene acylhydrazide class of virulence-blocking compounds. J Biol Chem 286:29922–29931
35. Wass MN, Kelley LA, Sternberg MJ (2010) 3DLigandSite: predicting ligand-binding sites using similar structures. Nucleic Acids Res 38:31
36. Tamura K, Stecher G, Peterson D, Filipski A, Kumar S (2013) MEGA6: molecular evolutionary genetics analysis version 6.0. Mol Biol Evol 30:2725–2729
37. Gasteiger E, Hoogland C, Gattiker A, Se Duvaud, Wilkins M, Appel R, Bairoch A (2005) Protein identification and analysis tools on the ExPASy Server. In: Walker J (ed) The proteomics protocols handbook. Humana Press, New York, pp 571–607
38. Franceschini A et al (2013) STRING v9.1: protein–protein interaction networks, with increased coverage and integration. Nucleic Acids Res 41:29
39. Geourjon C, Deleage G (1995) SOPMA: significant improvements in protein secondary structure prediction by consensus prediction from multiple alignments. Comput Appl Biosci 11:681–684
40. Xu D, Zhang Y (2011) Improving the physical realism and structural accuracy of protein models by a two-step atomic-level energy minimization. Biophys J 101:2525–2534
41. Ramachandran GN, Ramakrishnan C, Sasisekharan V (1963) Stereochemistry of polypeptide chain configurations. J Mol Biol 7:95–99
42. Eisenberg D, Luthy R, Bowie JU (1997) VERIFY3D: assessment of protein models with three-dimensional profiles. Methods Enzymol 277:396–404

43. Colovos C, Yeates TO (1993) Verification of protein structures: patterns of nonbonded atomic interactions. Protein Sci 2:1511–1519
44. Pontius J, Richelle J, Wodak SJ (1996) Deviations from standard atomic volumes as a quality measure for protein crystal structures. J Mol Biol 264:121–136
45. Wiederstein M, Sippl MJ (2007) ProSA-web: interactive web service for the recognition of errors in three-dimensional structures of proteins. Nucleic Acids Res 35:21
46. Hevener KE, Zhao W, Ball DM, Babaoglu K, Qi J, White SW, Lee RE (2009) Validation of molecular docking programs for virtual screening against dihydropteroate synthase. J Chem Inf Model 49:444–460
47. Hristozov DP, Oprea TI, Gasteiger J (2007) Virtual screening applications: a study of ligand-based methods and different structure representations in four different scenarios. J Comput Aided Mol Des 21:617–640
48. Osolodkin DI, Palyulin VA, Zefirov NS (2011) Structure-based virtual screening of glycogen synthase kinase 3beta inhibitors: analysis of scoring functions applied to large true actives and decoy sets. Chem Biol Drug Des 78:378–390
49. Pettersen EF, Goddard TD, Huang CC, Couch GS, Greenblatt DM, Meng EC, Ferrin TE (2004) UCSF Chimera—a visualization system for exploratory research and analysis. J Comput Chem 25:1605–1612
50. Dunbrack RL Jr (2002) Rotamer libraries in the 21st century. Curr Opin Struct Biol 12:431–440
51. Sanner MF (1999) Python: a programming language for software integration and development. J Mol Graph Model 17:57–61
52. Trott O, Olson AJ (2010) AutoDock Vina: improving the speed and accuracy of docking with a new scoring function, efficient optimization, and multithreading. J Comput Chem 31:455–461